

# Census of seafloor sediments in the world's ocean

Adriana Dutkiewicz<sup>1</sup>, R. Dietmar Müller<sup>1</sup>, Simon O'Callaghan<sup>2</sup>, and Hjörtur Jónasson<sup>1</sup>

<sup>1</sup>EarthByte Group, School of Geosciences, University of Sydney, Sydney, NSW 2006, Australia

<sup>2</sup>National ICT Australia (NICTA), Australian Technology Park, Eveleigh, NSW 2015, Australia

## ABSTRACT

**Knowing the patterns of distribution of sediments in the global ocean is critical for understanding biogeochemical cycles and how deep-sea deposits respond to environmental change at the sea surface. We present the first digital map of seafloor lithologies based on descriptions of nearly 14,500 samples from original cruise reports, interpolated using a support vector machine algorithm. We show that sediment distribution is more complex, with significant deviations from earlier hand-drawn maps, and that major lithologies occur in drastically different proportions globally. By coupling our digital map to oceanographic data sets, we find that the global occurrence of biogenic oozes is strongly linked to specific ranges in sea-surface parameters. In particular, by using recent computations of diatom distributions from pigment-calibrated chlorophyll-*a* satellite data, we show that, contrary to a widely held view, diatom oozes are not a reliable proxy for surface productivity. Their global accumulation is instead strongly dependent on low surface temperature (0.9–5.7 °C) and salinity (33.8–34.0 PSS, Practical Salinity Scale 1978) and high concentrations of nutrients. Under these conditions, diatom oozes will accumulate on the seafloor regardless of surface productivity as long as there is limited competition from biogenous and detrital components, and diatom frustules are not significantly dissolved prior to preservation. Quantifying the link between the seafloor and the sea surface through the use of large digital data sets will ultimately lead to more robust reconstructions and predictions of climate change and its impact on the ocean environment.**

## INTRODUCTION

Modern oceanic sediments cover 70% of the planet's surface, forming the substrate for the largest ecosystem on Earth and its largest carbon reservoir. The composition and distribution of sediments in the world's oceans underpins our understanding of global biogeochemical cycles, the occurrence of metal deposits, sediment transport mechanisms, the behavior of deep-ocean currents, reconstruction of past environments, and the response of the deep ocean to global warming. A comprehensive map of ocean sediments can help greatly in planning oceanographic expeditions, submarine search and recovery operations, and the assessment of geohazards and potential sites for the disposal of nuclear waste.

Virtually every marine geology and oceanography textbook contains a global map of five or six dominant sediment types in the ocean basins. Although there are many versions of this map (Barron and Whitman, 1981; Berger, 1976; Davies and Gorsline, 1976; Hüneke and Mulder, 2011; Trujillo and Thurman, 2014), they all show strikingly similar distributions of clays and calcareous and siliceous oozes, with large areas of the ocean basins draped in either pelagic red clay or lithogenous sediments (Fig. DR1 in the GSA Data Repository<sup>1</sup>). Despite the vast acquisition of new data, this hand-drawn map has changed very little since its inception (Berger, 1974). Here we present the first digital

map of recent sediments of the oceans based on carefully selected descriptions of surface sediment samples contained in cruise reports from recent expeditions and as long ago as the 1950s. The coupling of the sediment map to key oceanographic parameters provides new insights into the processes governing the distribution of sediments in the world's oceans and highlights several key discrepancies in the earlier maps.

## METHODOLOGY

Our map was created mostly using surface sample locations and descriptions obtained through the *Index to Marine and Lacustrine Geological Samples* (IMLGS) (Curators of Marine and Lacustrine Geological Samples Consortium, 2014). The IMLGS contains data on more than 200,000 marine sediment samples, the vast bulk of which postdates creation of the commonly used Deck41 data set (Bershad and Weiss, 1976) and the year (1983) of the last incarnation of the global map of oceanic sediments (Trujillo and Thurman, 2014). We selected 14,399 data points (Fig. 1) using strict quality control criteria (see the Data Repository).

There are many marine sediment classification schemes (Kennett, 1982) resulting in at least 80 different sediment types. The classification scheme that we use here is deliberately generalized in order to successfully depict the main types of sediments found in global oceans

and to overcome the shortcomings of inconsistent, poorly defined, and obsolete classification schemes and terminologies that are detailed in the majority of cruise reports. Our goal is to adhere to the classification scheme currently used by the International Ocean Discovery Program (Mazzullo et al., 1990), focusing on the descriptive aspect of the sediment rather than its genetic implications. As a result, we identify the following major classes of marine sediment (Fig. 1): gravel, sand, silt, clay, calcareous ooze, radiolarian ooze, diatom ooze, sponge spicules, mixed calcareous-siliceous ooze, shells and coral fragments, fine-grained calcareous sediment (not ooze), siliceous mud, and volcanoclastics (see the Data Repository).

The map is created using a support vector machine (SVM) (Cortes and Vapnik, 1995) classifier to predict the lithology in unobserved regions (see the Data Repository). The SVM is a nonparametric model that adapts in complexity as new data are added. To reduce the risk of overfitting to the measurements at the expense of the model's ability to generalize into areas outside of the sampled regions, a cross-validation approach was employed to train the classifier. This approach maximizes the model's accuracy on observations that are withheld from the training set. For prediction, a one-against-one method (Bishop, 2006) was used to address the problem of modeling multiple classes with a bilinear classifier. Classes were weighted inversely proportional to their number of recorded instances to account for the unbalanced nature of the data. Deep-sea lithologies that collectively compose >70% of seafloor sediment have been predicted with very high accuracy (to 80%) (Figs. DR2–DR4).

## RESULTS

Our digital map (Fig. 2) reveals that the pattern of distribution of different lithologies is more complex, with significant regional deviations from earlier maps (Barron and Whitman, 1981; Berger, 1976; Davies and Gorsline, 1976; Hüneke and Mulder, 2011; Trujillo and Thurman, 2014) (Fig. DR1). The lithologies occur in drastically different proportions globally (Table DR1); coverage by calcareous sediment and clay each increased by ~30%, and that of diatom and radiolarian oozes decreased by ~25%

<sup>1</sup>GSA Data Repository item 2015271, descriptions of sample selection criteria and lithology classes, support vector machine classifier, oceanographic datasets, Figures DR1–DR8, and Tables DR1 and DR2, is available online at [www.geosociety.org/pubs/ft2015.htm](http://www.geosociety.org/pubs/ft2015.htm), or on request from [editing@geosociety.org](mailto:editing@geosociety.org) or Documents Secretary, GSA, P.O. Box 9140, Boulder, CO 80301, USA. Gridded data are available at [ftp://ftp.earthbyte.org/papers/Dutkiewicz\\_et\\_al\\_seafloor\\_lithology/](http://ftp.earthbyte.org/papers/Dutkiewicz_et_al_seafloor_lithology/), and can be viewed on an interactive 3-D globe at <http://portal.gplates.org/cesium/?view=seabed>.

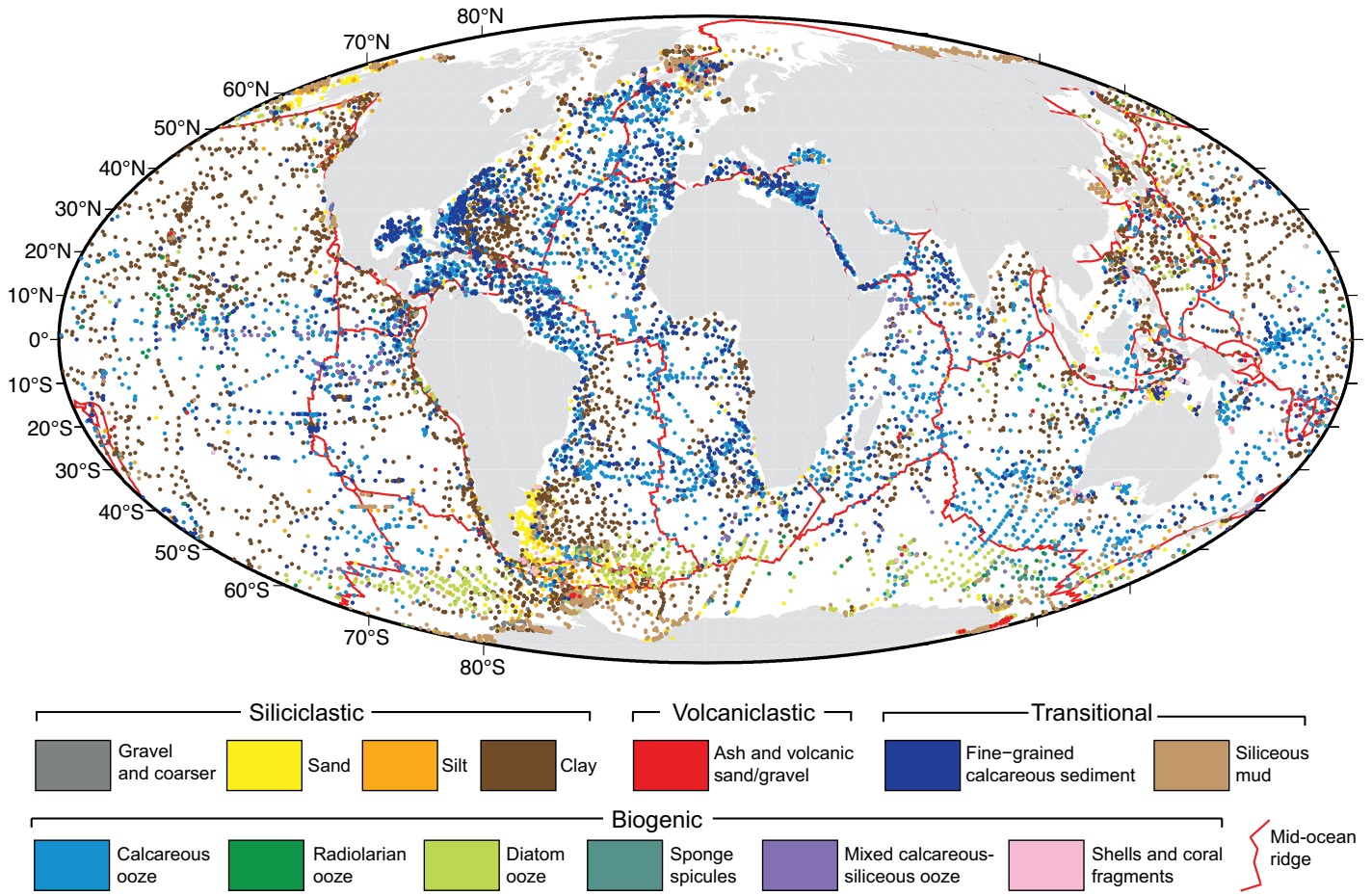


**Figure 1.** Seafloor sediment sample locations. Lithology-coded sample locations of surface sediments ( $n = 14,399$ ) used to create the digital map of seafloor sediments in world's ocean basins (Fig. 2). Mollweide projection.

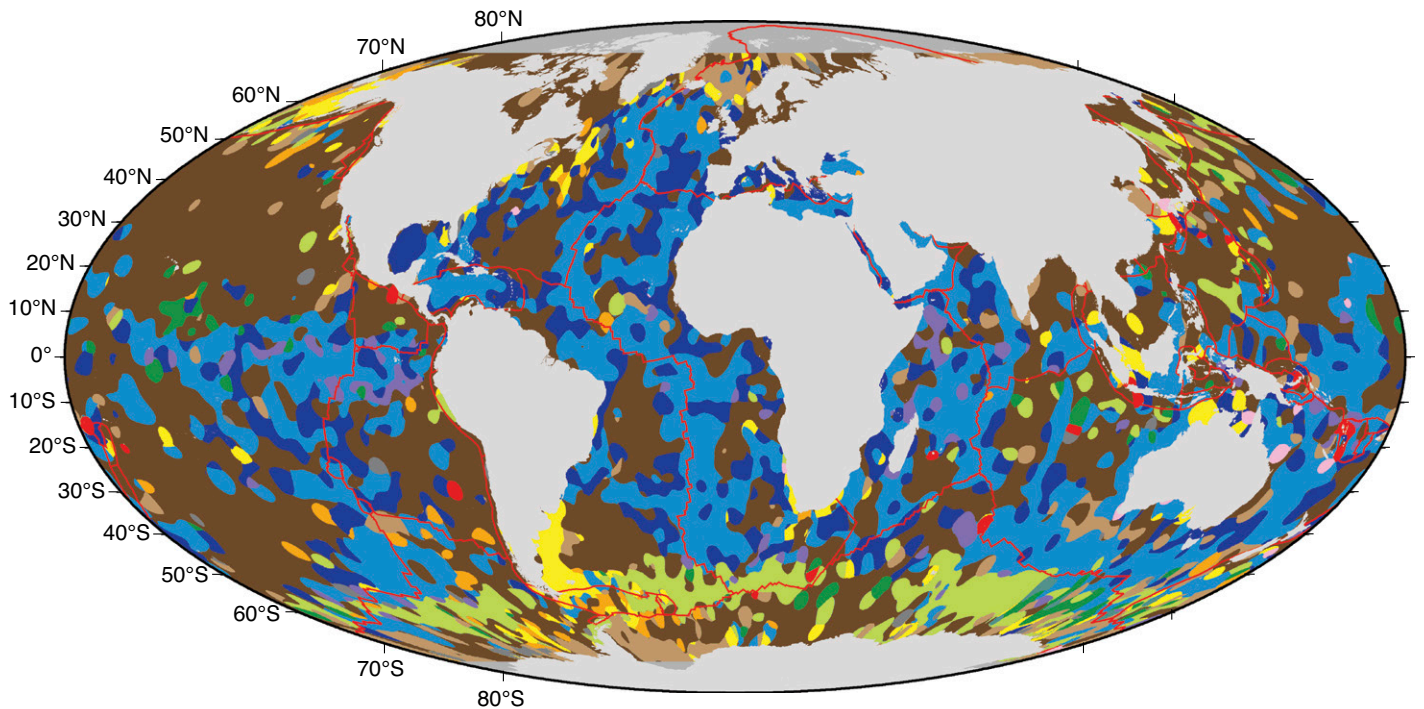


**Figure 2.** Digital map of major lithologies of seafloor sediments in world's ocean basins. Legend is the same as in Figure 1. More detailed views of major ocean basins and percentage estimates of lithologies are given in Figures DR4B–DR4E and Table DR1 (see footnote 1). Mollweide projection.

and 60%, respectively. Rather than forming a belt in the equatorial Pacific extending to 30°S along the west coast of South America (Fig. DR1), radiolarian oozes occur as isolated pockets around the equatorial Pacific in association with patches of mixed oozes and as a component of diatom ooze within the Peru Basin (Fig. 2). This is also the case in the Atlantic and Indian Oceans, where radiolarian oozes are mixed with calcareous and diatom oozes. Patches of radiolarian ooze are, however, common in the Southern Ocean; this is not apparent on pre-existing maps. There are numerous large areas of diatom ooze within predominant clay lithology in the northern Pacific and central Indian Oceans. The circum-Antarctic belt of diatom ooze is discontinuous on our map, with a major interruption in the Drake Passage, where sedimentation is dominated by a large body of sand (Fig. 2). Sponge spicules form a significant component of seafloor sediment in parts of the Australian-Antarctic Basin where they co-occur with diatom and radiolarian oozes. Compared to earlier maps clay occupies a considerably larger area around eastern and western South America and is significantly more abundant in the Indian Ocean, where its southern extent from the Bengal Fan is interrupted only by the Ninetyeast and Broken ridges. Clay is dominant within the South Australia Basin (Fig. 2) but does not spread into the Southern Ocean, as shown on older maps (Fig. DR1).

## DISCUSSION

Marine planktonic organisms play a critical role in the global cycling of silica and carbon and in the biological pump of CO<sub>2</sub> (Ragueneau et al., 2000). However, many of the mechanisms that are thought to control the geologic accumulation of biogenic carbonate and silica are very difficult to quantify, even on a local scale (e.g., Broecker, 2008; Ragueneau et al., 2000). Our digital map of seafloor sediments provides a missing link for constraining global relationships between the source (sea surface), for which comprehensive data sets exist (see the Data Repository), and the sink (seafloor). Here we focus on diatoms, because their predominance in the Southern Ocean, where they are estimated to contribute as much as 75% of the total primary productivity (Crosta et al., 2005), and their subsequent preservation on the seafloor have been particularly controversial (e.g., Nelson et al., 2002, 1995; Pondaven et al., 2000). We find that the bulk of diatom oozes occurs at seafloor depths of 3300–4800 m, below surface water that has very restricted and low temperatures (0.9–5.7 °C), consistent with, but slightly narrower than, the 0.8–8 °C range required for optimal diatom growth in the Southern Ocean (Neori and Holm-Hansen, 1982). The salinity range of these surface waters is low and narrow (33.8–34.0 PSS, Practical Salinity Scale 1978), which according to experiments reduces

dissolution of biogenic SiO<sub>2</sub> relative to typical seawater salinity (Roubeix et al., 2008). The summer productivity is modest (230–840 mgC/m<sup>2</sup>/day in the Northern Hemisphere and 175–260 mgC/m<sup>2</sup>/day in the Southern Hemisphere), based on satellite-derived surface chlorophyll-*a* concentrations, and in the Southern Ocean may be limited by iron and light (e.g., Claquin et al., 2002). Diatom oozes are associated with the highest and narrowest ranges of surface nutrients, especially growth-limiting silicate (Martin-Jézéquel et al., 2000), of all lithology classes including siliceous radiolarian oozes (Figs. DR4–DR6; Table DR2).

Recent computations of global distributions of phytoplankton species from chlorophyll-*a* satellite data calibrated with in situ measurements of diagnostic pigments (Hirata et al., 2011) show that diatoms are a major contributor to primary productivity in the Southern Ocean, and peak in numbers in the austral summer (Soppa et al., 2014). However, even with these vastly improved maps of diatom abundances that capture seasonal blooms, we fail to find a strong link between diatom chlorophyll concentration and diatom ooze occurrence (Fig. 3; Fig. DR7). Diatom ooze association with high diatom chlorophyll concentrations in the north Weddell Sea and around Prydz Bay is an exception, not the rule. Diatom ooze is most common below waters with very low diatom chlorophyll concentration, forming prominent zones between 50°S and 60°S in the Australian-Antarctic and the Bellinghausen basins (Fig. 3). These large-scale patterns cannot be easily explained by post-depositional sediment redistribution (Dezileau et al., 2000) and contradict the widely held view, based on hydrographic and sediment trap data,

that biogenic opal accumulation in the Southern Ocean is linked to high surface productivity (e.g., Nelson et al., 2002; Pondaven et al., 2000). As biogenic silica preservation efficiency, estimated to be a mere 1.2%–5.5% (Nelson et al., 2002), is no longer considered critical for diatom accumulation in the Southern Ocean (Nelson et al., 2002, 1995; Pondaven et al., 2000), we propose that the accumulation of diatom oozes is strongly dependent on limited competition from biogenous and lithogenous components. Diatoms are conspicuously absent below the prominent 40°S diatom chlorophyll concentration belt (Fig. 3). The belt coincides with a marked northward increase in salinity and temperature and a decrease in dissolved silicate (Fig. DR8) conducive for the proliferation of biocalcareous organisms and the subsequent accumulation of calcareous oozes on the seafloor above the carbonate compensation depth (Broecker, 2008) (Fig. 3; Fig. DR7). Likewise, diatom oozes are absent below high diatom chlorophyll areas near continents, where their presence in the sediment is diluted by terrigenous input. This suggests that the occurrence of diatom oozes is not a reliable indicator of diatom paleoproductivity and that it is strongly dependent on sea-surface parameters that collectively inhibit the growth and overpopulation by competing organisms such as calcifying plankton.

## CONCLUSIONS

Our digital map of recent ocean sediments reveals that the seafloor is draped in a complex patchwork of lithologies where previously large continuous regions or belts were mapped. By coupling the map to existing oceanographic data sets we are able to quantify the relationship

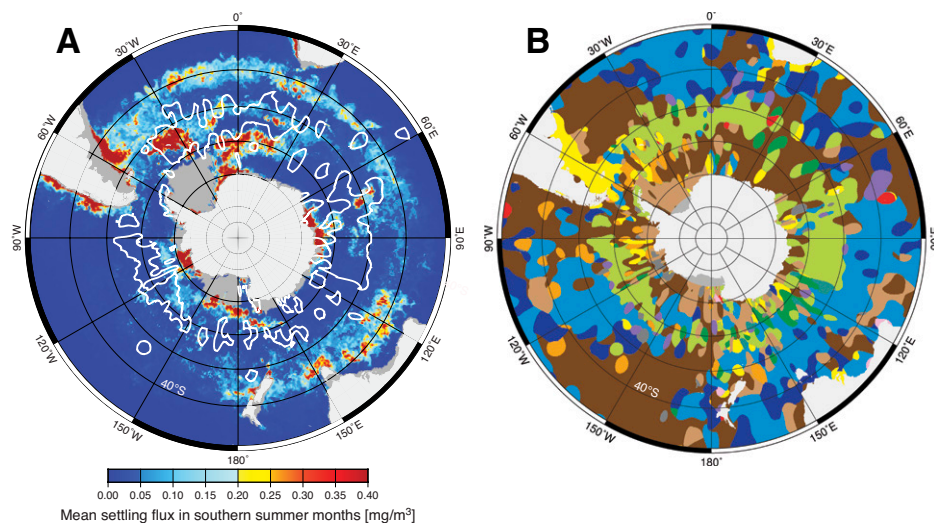


**Figure 3. Biosiliceous oozes versus diatom chlorophyll concentration in the Southern Ocean. Stereographic projection. A:** Outlines (in white) of regions where we map diatom oozes superimposed on austral summer average of diatom chlorophyll concentrations (mg/m<sup>3</sup>) for the period 2003–2013 (Soppa et al., 2014). Color scale highlights subtle variations in diatom chlorophyll concentration; maxima (dark red) reach ~18 mg/m<sup>3</sup>. **B:** Distribution of lithologies; legend as in Figure 1.



between various sea-surface parameters and directly underlying seafloor sediment type on a global scale. We conclude that diatom ooze is not a reliable proxy for surface productivity, but it is a good indicator of sea-surface oceanographic variables (Cunningham and Leventer, 1998), especially temperature (Romero et al., 2005; Zielinski and Gersonde, 1997) and nutrients (Chisholm, 1992; Martin-Jézéquel et al., 2000). Diatom ooze will accumulate under restricted conditions even when surface productivity is low, provided that there are no dominant competing components such as nanoplankton (Hirata et al., 2011) and diatom-grazing radiolarians (Hüneke and Mulder, 2011), and provided that diatom frustules are not significantly dissolved in the water column or on the seafloor (Nelson et al., 1995; Ragueneau et al., 2000; Tréguer and De La Rocha, 2013). Our seafloor lithology map is a new digital, open-access resource that provides a basis for elucidating global relationships between the sedimentary record and a variety of oceanographic parameters, providing additional constraints for models of paleoproductivity and global biogeochemical cycles.

#### ACKNOWLEDGMENTS

We are grateful to cruise participants and the curators of the Index to Marine and Lacustrine Geological Samples at the U.S. *National Oceanic and Atmospheric Administration*. We thank Mariana Soppa for the diatom chlorophyll data set, and Clark Alexander and Charlotte Sjunneskog for access to additional sample descriptions. We thank Maria Seton, Paul Wessel, Alan P. Trujillo, an anonymous reviewer, and editor Ellen Thomas for their thorough reviews. This research was supported by the Australian Science Industry Endowment Fund (RP 04-174) Big Data Knowledge Discovery project.

#### REFERENCES CITED

- Barron, E.J., and Whitman, J.M., 1981, Oceanic sediments in space and time, in Emiliani, C., ed., *The Sea, Volume 7*: New York, Wiley Interscience, p. 689–733.
- Berger, W.H., 1974, Deep-sea sedimentation, in Burk, C.A., and Drake, C.D., eds., *The geology of continental margins*: New York, Springer-Verlag, p. 213–241.
- Berger, W.H., 1976, Biogenous deep sea sediments: Production, preservation and interpretation, in Riley, J.P., and Chester, R., eds., *Chemical oceanography, Volume 5*: London, Academic Press, p. 265–389.
- Bershad, S., and Weiss, M., 1976, Deck41 surficial seafloor sediment description database: National Geophysical Data Center, National Oceanic and Atmospheric Administration, doi:10.7289/V5VD6WCZ.
- Bishop, C.M., 2006, Pattern recognition and machine learning: New York, Springer-Verlag, 738 p.
- Broecker, W.S., 2008, A need to improve reconstructions of the fluctuations in the calcite compensation depth over the course of the Cenozoic: *Paleoceanography*, v. 23, PA1204, doi:10.1029/2007PA001456.
- Chisholm, S.W., 1992, Phytoplankton size, in Falkowski, P.G., and Woodhead, A.D., eds., *Primary productivity and biogeochemical cycles in the sea*: New York, Plenum, p. 213–237.
- Claquin, P., Martin-Jézéquel, V., Kromkamp, J.C., Veldhuis, M.J.W., and Kraay, G.W., 2002, Uncoupling of silicon compared with carbon and nitrogen metabolisms and the role of the cell cycle in continuous cultures of *Thalassiosira pseudonana* (Bacillariophyceae) under light, nitrogen, and phosphorus control: *Journal of Phycology*, v. 38, p. 922–930, doi:10.1046/j.1529-8817.2002.t01-1-01220.x.
- Cortes, C., and Vapnik, V., 1995, Support-vector networks: *Machine Learning*, v. 20, p. 273–297, doi:10.1007/BF00994018.
- Crosta, X., Romero, O., Armand, L.K., and Pichon, J.-J., 2005, The biogeography of major diatom taxa in Southern Ocean sediments: 2. Open ocean related species: *Palaeogeography, Palaeoclimatology, Palaeoecology*, v. 223, p. 66–92, doi:10.1016/j.palaeo.2005.03.028.
- Cunningham, W.L., and Leventer, A., 1998, Diatom assemblages in surface sediments of the Ross Sea: Relationship to present oceanographic conditions: *Antarctic Science*, v. 10, p. 134–146, doi:10.1017/S0954102098000182.
- Curators of Marine and Lacustrine Geological Samples Consortium, 2015, Index to Marine and Lacustrine Geological Samples (IMLGS): National Geophysical Data Center, National Oceanic and Atmospheric Administration, doi:10.7289/V5H41PBB.
- Davies, T.A., and Gorsline, D.S., 1976, The geochemistry of deep-sea sediments, in Riley, J.P., and Chester, R., eds., *Chemical oceanography, Volume 5*: London, Academic Press, p. 1–80.
- Dezileau, L., Bareille, G., Reyss, J.L., and Lemoine, F., 2000, Evidence for strong sediment redistribution by bottom currents along the southeast Indian Ridge: *Deep-Sea Research. Part I, Oceanographic Research Papers*, v. 47, p. 1899–1936, doi:10.1016/S0967-0637(00)00008-X.
- Hirata, T., Hardman-Mountford, N.J., Brewin, R.J.W., Aiken, J., Barlow, R., Suzuki, K., Isada, T., Howell, E., Hashioka, T., and Noguchi-Aita, M., 2011, Synoptic relationships between surface Chlorophyll-*a* and diagnostic pigments specific to phytoplankton functional types: *Biogeosciences*, v. 8, p. 311–327, doi:10.5194/bg-8-311-2011.
- Hüneke, H., and Mulder, T., 2011, *Deep-sea sediments*: Amsterdam, Elsevier, 849 p.
- Kennett, J., 1982, *Marine geology*: Englewood Cliffs, New Jersey, Prentice Hall, 813 p.
- Martin-Jézéquel, V., Hildebrand, M., and Brzezinski, M.A., 2000, Silicon metabolism in diatoms: Implications for growth: *Journal of Phycology*, v. 36, p. 821–840, doi:10.1046/j.1529-8817.2000.00019.x.
- Mazzullo, J., Meyer, A., and Kidd, R., 1990, Appendix B. New sediment classification scheme, in Rabinowitz, P.D., et al., eds., *Shipboard scientists' handbook: Ocean Drilling Program Technical Note 3*: College Station, Texas, Ocean Drilling Program, p. 125–140.
- Nelson, D.M., Tréguer, P., Brzezinski, M.A., Leynaert, A., and Quéguiner, B., 1995, Production and dissolution of biogenic silica in the ocean: Revised global estimates, comparison with regional data and relationship to biogenic sedimentation: *Global Biogeochemical Cycles*, v. 9, p. 359–372, doi:10.1029/95GB01070.
- Nelson, D.M., Anderson, R.F., Barber, R.T., Brzezinski, M.A., Buesseler, K.O., Chase, Z., Collier, R.W., Dickson, M.-L., François, R., and Hiscock, M.R., 2002, Vertical budgets for organic carbon and biogenic silica in the Pacific sector of the Southern Ocean, 1996–1998: *Deep-Sea Research. Part II, Topical Studies in Oceanography*, v. 49, p. 1645–1674, doi:10.1016/S0967-0645(02)00005-X.
- Neori, A., and Holm-Hansen, O., 1982, Effect of temperature on rate of photosynthesis in Antarctic phytoplankton: *Polar Biology*, v. 1, p. 33–38, doi:10.1007/BF00568752.
- Pondaven, P., Ragueneau, O., Tréguer, P., Hauvespre, A., Dezileau, L., and Reyss, J.L., 2000, Resolving the 'opal paradox' in the Southern Ocean: *Nature*, v. 405, p. 168–172, doi:10.1038/35012046.
- Ragueneau, O., Tréguer, P., Leynaert, A., Anderson, R.F., Brzezinski, M.A., DeMaster, D.J., Dugdale, R.C., Dymond, J., Fischer, G., and Francois, R., 2000, A review of the Si cycle in the modern ocean: Recent progress and missing gaps in the application of biogenic opal as a paleoproductivity proxy: *Global and Planetary Change*, v. 26, p. 317–365, doi:10.1016/S0921-8181(00)00052-7.
- Romero, O.E., Armand, L.K., Crosta, X., and Pichon, J.J., 2005, The biogeography of major diatom taxa in Southern Ocean surface sediments: 3. Tropical/subtropical species: *Palaeogeography, Palaeoclimatology, Palaeoecology*, v. 223, p. 49–65, doi:10.1016/j.palaeo.2005.03.027.
- Roubeix, V., Becquevort, S., and Lancelot, C., 2008, Influence of bacteria and salinity on diatom biogenic silica dissolution in estuarine systems: *Biogeochemistry*, v. 88, p. 47–62, doi:10.1007/s10533-008-9193-8.
- Soppa, M.A., Hirata, T., Silva, B., Dinter, T., Peeken, L., Wiegmann, S., and Bracher, A., 2014, Global retrieval of diatom abundance based on phytoplankton pigments and satellite data: *Remote Sensing*, v. 6, p. 10,089–10,106, doi:10.3390/rs61010089.
- Tréguer, P.J., and De La Rocha, C.L., 2013, The world ocean silica cycle: *Annual Review of Marine Science*, v. 5, p. 477–501, doi:10.1146/annurev-marine-121211-172346.
- Trujillo, A.P., and Thurman, H.V., 2014, *Essentials of oceanography* (eleventh edition): Upper Saddle River, New Jersey, Prentice Hall, 608 p.
- Zielinski, U., and Gersonde, R., 1997, Diatom distribution in Southern Ocean surface sediments (Atlantic sector): Implications for paleoenvironmental reconstructions: *Palaeogeography, Palaeoclimatology, Palaeoecology*, v. 129, p. 213–250, doi:10.1016/S0031-0182(96)00130-7.

Manuscript received 12 April 2015  
 Revised manuscript received 24 June 2015  
 Manuscript accepted 28 June 2015

Printed in USA